NURETH14-151

COMPARATIVE ANALYSIS OF CTF AND TRACE THERMAL-HYDRAULIC CODES USING OECD/NRC PSBT BENCHMARK VOID DISTRIBUTION DATABASE M. Avramova¹, A. Velazquez-Lozada² and A. Rubin¹

¹The Pennsylvania State University, University Park, PA, USA ²US Nuclear Regulatory Commission, Washington, DC, USA

mna109@psu.edu, Alexander.Velazquez-Lozada@nrc.gov, ajr5052@psu.edu

Abstract

The international OECD/NRC PWR Subchannel and Bundle Tests (PSBT) benchmark has been established to provide a test bed for assessing the capabilities of various thermal-hydraulic subchannel, system, and computational fluid dynamics (CFD) codes and to encourage advancement in the analysis of fluid flow in rod bundles. The aim is to improve the reliability of the nuclear reactor safety margin evaluations. The benchmark is based on one of the most valuable databases identified for the thermal-hydraulics modeling, which was developed by the Nuclear Power Engineering Corporation (NUPEC) in Japan. The database includes subchannel void fraction and departure from nucleate boiling (DNB) measurements in a representative Pressurized Water Reactor (PWR) fuel assembly. Part of this database is made available for the international PSBT benchmark activity.

The PSBT benchmark team is organized based on the collaboration between the Pennsylvania State University (PSU) and the Japan Nuclear Energy Safety organization (JNES) including the participation and support of the U.S. Nuclear Regulatory Commission (NRC) and the Nuclear Energy Agency (NEA), OECD.

On behalf of the PSBT benchmark team, PSU in collaboration with US NRC is performing supporting calculations of the benchmark exercises using its in-house advanced thermal-hydraulic subchannel code CTF and the US NRC system code TRACE.

CTF is a version of the well-known and widely used code COBRA-TF whose models have been continuously improved and validated over the last years at the Reactor Dynamics and Fuel Management Group (RDFMG) at PSU.

TRACE is a reactor systems code developed by the U.S. Nuclear Regulatory Commission to analyze transient and steady-state thermal-hydraulic behavior in Light Water Reactors (LWRs) and it has been designed to perform best-estimate analyses of loss-of-coolant accidents (LOCAs), operational transients, and other accident scenarios in PWRs and boiling light-water reactors (BWRs).

The paper presents the CTF and TRACE models for the exercises of the void distribution phase of the OECD/NRC PSBT benchmark. Code-to-code and code-to-data comparisons are provided along with a discussion of the void generation and void distribution models available in the two codes.

1. Introduction

In the past few decades, the need of improved nuclear reactor safety analyses has led to a rapid development of advanced methods for multidimensional thermal-hydraulic analyses. These methods have progressively become more complex in order to account for variety of physical phenomena anticipated during steady-state and transient Light Water Reactor (LWR) conditions. The newly developed models must be extensively validated against full-scale high quality experimental data. In that sense, the ongoing OECD/NRC PWR Subchannel and Bundle Tests (PSBT) benchmark [1] provides an excellent opportunity for validation of innovative models for void distribution and departure from nucleate boiling (DNB) prediction under Pressurized Water Reactors (PWRs) conditions. From 1980s to 1990s, NUPEC (Nuclear Power Engineering Corporation) performed a series of void measurement tests using full-size mock-up tests for both Boiling Water Reactors (BWRs) and PWRs. Based on stateof-the-art computer tomography (CT) technology, the void distribution was visualized at the mesh size smaller than the subchannel under actual plant conditions. NUPEC also performed steady state and transient critical power test series based on the equivalent full-size mock-ups. Considering the reliability not only of the measured data, but also other relevant parameters such as the system pressure, inlet sub-cooling and rod surface temperature, these test series supply the first substantial database for the development of truly mechanistic and consistent models for void distribution and departure from nucleate boiling.

CTF is a version of the COBRA-TF code maintained at the Reactor Dynamics and Fuel Management Group (RDFMG) at the Pennsylvania State University (PSU) [2]. The original version of COBRA-TF was developed at the Pacific Northwest Laboratory as a part of the COBRA/TRAC thermal-hydraulic code. Since then, various academic and industrial organizations have adapted, developed and modified the code in many directions. The code is worldwide used for academic and general research purposes as well. The code version used at PSU originates from a code version modified during the FLECHT SEASET program [3]. Besides the code utilization to teach and train students in the area of nuclear reactor thermalhydraulic safety analyses, during the last few years at PSU the theoretical models and numerics of COBRA-TF were substantially improved [4]. The code was subjected to an extensive verification and validation program and was applied to variety of LWR steady state and transient simulations. CTF is a transient code based on a separated flow representation of the two-phase flow. The two-fluid formulation, generally used in thermal-hydraulic codes, separates the conservation equations of mass, energy, and momentum to vapor and liquid. CTF extends this treatment to three fields: vapor, continuous liquid and entrained liquid droplets, which results in a set of nine time-averaged conservation equations. The conservation equations for each of the three fields and for heat transfer from and within the solid structure in contact with the fluid are solved using a semi-implicit, finite-difference numerical technique on an Eulerian mesh, where time intervals are assumed to be long enough to smooth out the random fluctuations in the multiphase flow, but short enough to preserve any gross flow unsteadiness. The code is able to handle both hot wall and normal flow regimes maps and it is capable of calculating reverse flow, counter flow, and crossflow situations. The code is developed for use with either 3D Cartesian or subchannel coordinates and, therefore, it features extremely flexible nodding for both the thermal-hydraulic and the heat-transfer solution. This flexibility allows a fully 3D treatment in geometries amenable to description in a Cartesian coordinate system.

TRACE is a multi-component solver consolidation of four US NRC computer codes: TRAC-P, TRAC-B, RELAP5 and RAMONA. TRACE has been validated and assessed against more than 500 experimental sets of data from separate and integral effects tests, which comparisons were found to be reasonable in general [5]. TRACE utilizes a finite-volume technique to discretize typical hydraulic components found in a nuclear power plant and calculates the internal energy and equations of motion in each component for two-phases. The energy equation is solved using a semi-implicitly numerical-scheme and the equations of fluid-motion are solve using the stability-enhancing two-step (SETS) numerical-scheme which allows the material Courant limit to be exceeded. This allows very large time steps to be used in slow transients. This set of equations is solved for one and three dimensions in Cartesian and/or cylindrical coordinates. Errors introduced to the solution due to abrupt area changes are corrected by modifying the equations of motion to force Bernoulli flow.

The following two sections discuss the void generation and distribution models available in CTF and TRACE with a subsequent code-to-code and code-to-data comparison.

2. **CTF Models for Vapor Generation and Distribution**

The three-field formulation of the two-phase flow used in CTF is a straightforward extension of the general two-fluid model. Dividing the liquid phase into a continuous liquid field and an entrained liquid drop field allows both fields to have different velocities. The generalized phasic momentum equation is then given as:

$$\frac{\partial}{\partial t} \left(\alpha_k \rho_k \underline{U}_k \right) + \nabla \cdot \left(\alpha_k \rho_k \underline{U}_k \underline{U}_k \right) = \alpha_k \rho_k g - \alpha_k \nabla P + \nabla \cdot \left(\alpha_k \frac{\tau}{z_k} \right) + M_k^T + M_k^d + M_k^T, \tag{1}$$

where α_k is the average k-phase void fraction; ρ_k is the average k-phase density; \underline{U}_k is the average k-phase velocity vector; g is the acceleration of gravity vector; $\underline{\tau}_k$ is the average k-phase viscous stress tensor; M_k^T is the average supply of momentum to phase k due to mass transfer to phase k; M_k^d is the average drag force on phase k by the other phases; M_k^T is the average supply of momentum to phase k due to turbulent mixing and void drift.

In the generalized phasic momentum equation the terms representing the momentum exchange at the interface (interfacial momentum terms) are expressed as:

$$\underline{M}_{vap}^{d} = -\underline{\tau}_{i,vap_liq}^{"} - \underline{\tau}_{i,vav_ent}^{"} - \text{vapor phase},$$
 (2a)

$$\underline{M}_{liq}^{d} = \underline{\tau}_{i,vap_liq}^{"} - \text{continuous liquid phase,}$$
 (2b)

$$\underline{\underline{M}}_{ent}^d = \underline{\underline{\tau}}_{i,vap\ ent}^{""}$$
 - entrained liquid phase, (2c)

where $\underline{\tau}_{i,vap_liq}^{'''}$ is the average drag force per unit volume by the vapor on the continuous liquid and $\underline{\tau}_{i,vap_ent}^{m}$ is the average drag force per unit volume by the vapor on the entrained liquid.

The momentum exchange due to mass transfer between the three fields can be written as:

$$\underline{M}_{vap}^{\Gamma} = \left(\Gamma^{"'}\underline{U}\right) \qquad - \text{ vapor phase,} \tag{3a}$$

$$\underline{M}_{liq}^{\Gamma} = -\left(\Gamma_{liq}^{"}\underline{U}\right) - \left(S^{"}\underline{U}\right) - \text{continuous liquid phase,} \tag{3b}$$

$$\underline{M}_{ent}^{\Gamma} = -\left(\Gamma_{ent}^{"}\underline{U}\right) + \left(S^{"}\underline{U}\right) - \text{entrained liquid phase,}$$
(3c)

where the $\Gamma^{'''}$ is the average rate of vapor generation per unit volume and $S^{'''}$ is the average net rate of entrainment per unit volume. Since both liquid fields contribute to the vapor generation, then $\Gamma^{'''} = \Gamma^{'''}_{liq} + \Gamma^{'''}_{ent}$.

If η denotes the fraction of the total vapor generation coming from the entrained liquid field, then

$$\Gamma_{vap}^{"'} = \Gamma^{"'},$$
 (4a)

$$\Gamma_{ent}^{"} = \eta \Gamma^{"} = -\Gamma_{ent}^{"} + S^{"} = -\eta \Gamma^{"} + S^{"},$$
(4b)

and

$$\Gamma_{liq}^{"} = (1 - \eta)\Gamma^{"} = -\Gamma_{liq}^{"} - S^{"} = -(1 - \eta)\Gamma^{"} - S^{"}.$$
(4c)

The momentum exchange due to turbulent mixing and void drift is neglected in the entrained liquid field in the annular flow regime:

$$M_{ent}^T = 0 \text{ if } \alpha_{vap} \ge 0.8.$$

Also, the viscous stress is partitioned into a wall shear and a fluid-fluid shear; the fluid-fluid shear is neglected:

$$\nabla \cdot \left(\alpha_k \, \underline{\underline{\tau}}_k\right) = \underline{\underline{\tau}}_{wall,k}^{"} .$$

The model for interfacial mass transfer is obtained from the energy jump condition by neglecting the mechanical terms and averaging:

$$\Gamma^{"} = \frac{-q_{I_l}^{"} - q_{I_v}^{"}}{h_{f_o}} \tag{5}$$

The interfacial heat transfer, $q_I^{"}$, for phase k is given by

$$q_{I_k}^{"} = hA_I^{"}(T_s - T_k) \tag{6}$$

where $A_I^{"}$ is the average interfacial area per unit volume and h is a surface heat transfer coefficient. The vapor generation is divided into four components, two for each phase, depending on whether the phase is superheated or subcooled and the total vapor generation rate is given by the sum of these components. The interfacial area per unit volume, $A_I^{"}$, is based on the flow regime, as are the heat transfer coefficients, h.

The interfacial drag force per unit volume between any two fields is assumed to be a function of the relative velocity between both fields. The interfacial friction coefficients are flow regime dependent and, therefore, neither void correlation nor two-phase pressure drop correlation has to be applied. Interfacial drag forces are modeled between continuous liquid and disperse vapor in the bubbly flows and between continuous liquid film and vapor core and entrained droplets and vapor core in the annular flow. The treatment of the interfacial drag is described in Table I.

Turbulent mixing and void drift phenomena are modeled in CTF by the Lahey and Moody approach [6], where the net two-phase mixing (including void drift) is assumed to be proportional to the non-equilibrium void fraction gradient. The void drift is only assumed to occur in bubbly, slug, and churn flow, where liquid is the continuous phase and vapor is the dispersed phase. The single phase mixing coefficient can be either specified as an input value or calculated using an empirical correlation derived by Rogers and Rosehart [7]. The Beus' model for two-phase turbulent mixing is utilized [8]. In 1980s, both approaches were representing the state-of-art in turbulent mixing and void drift modeling. Nowadays they are still used in the most of the subchannel codes. A detailed description of the current CTF turbulent mixing and void drift models is given in Table II.

Table I. CTF Modeling of the Interfacial Drag

Interfacial Drag Forces	Between continuous liquid and vapor: $ au_{I,vap_liq} = K_{I,vap_liq} U_{vap_liq}$
	Between entrained liquid and vapor: $\tau_{I,vap_ent} = K_{I,vap_ent}U_{vap_ent}$
Interfacial Drag Coefficients	Bubbly Flows For small bubbles: $K_{I,vap_liq} = 0.375 \frac{C_{D_{bub}}}{r_{bub}} \alpha_{vap} \rho_{liq} \big U_{vap} - U_{liq} \big ; \qquad C_{D_{bub}} = \frac{24}{\text{Re}_{bub}} \left(1 + 0.1 \text{Re}_{bub}^{0.75} \right)$ For large bubbles: $K_{I,vap_liq} = 0.375 \frac{C_{D_{lbub}}}{r_{bub}} \alpha_{vap} \rho_{liq} \big U_{vap} - U_{liq} \big ; C_{D_{lbub}} = \max \left(\frac{24}{\text{Re}_{Lbub}} \left(1 + 0.1 \text{Re}_{Lbub}^{0.75} \right) \alpha_{liq}^2, 0.45 \alpha_{liq}^2 \right)$ Annular Flow Between continuous liquid film and vapor core: $K_{I,vap_liq} = 2 \frac{f_I}{D_{hyd}} \sqrt{\alpha_{vap} + \alpha_{ent}} \rho_{vap} \big U_{vap} - U_{liq} \big ; \text{ interfacial friction factor } f_I \text{ by Henstoch and Hanratty}$ Between entrained liquid film and vapor core:
	$K_{I,vap_drop} = 0.375 \frac{C_{D_{drop}}}{r_{drop}} \alpha_{ent} \rho_{vap} U_{vap} - U_{ent} ; C_{D_{drop}} = \frac{24}{\text{Re}_{drop}} (1 + 0.1 \text{Re}_{drop}^{0.75})$

Table II. CTF Models for Turbulent Mixing and Void Drift

	Mass exchange of the phase k : $\dot{m}_{k}^{TM} = -\beta_{TP} \frac{\overline{G}}{\overline{\rho}} (\alpha_{k,j} \rho_{k,j} - \alpha_{k,i} \rho_{k,i})$			
Turbulent Mixing	Momentum exchange of the phase k : $\dot{I}_{k}^{TM} = -\beta_{TP} \frac{\overline{G}}{\overline{\rho}} \Delta G_{k} A$			
	Energy exchange of the phase k : $\dot{Q}_k^{TM} = -\beta_{TP} \frac{\overline{G}}{\overline{\rho}} \Delta(\alpha_k \rho_k h_k) A$			
	User specified single value based on experimental data			
Single-	or			
Phase	Internally calculated using the correlation by Rogers & Rozehart:			
Turbulent				
Mixing Coefficient	$\beta_{\rm SP} = \frac{1}{2} 0.0058 \left(\frac{D_{\rm gap}}{D_{\rm rod}} \right)^{-1.46} Re^{-0.1} \left[1 + \left(\frac{D_{\rm hyd,i}}{D_{\rm hyd,i}} \right)^{1.5} \right] \frac{D_{\rm hyd,i}}{D_{\rm rod}}$			
	Two-phase multiplier by Beus: $\beta_{TP} = \Theta_{TP} \beta_{SP}$;			
Two-Phase Turbulent Mixing Coefficient	$\Theta_{\text{TP}} = 1 + (\Theta_{\text{max}} - 1) \frac{x}{x_{\text{max}}} \text{ if } x \leq x_{\text{max}}$			
	$\Theta_{\text{TP}} = 1 + (\Theta_{\text{max}} - 1) \frac{x_{\text{max}} - x_0}{x - x_0} \text{ with } \frac{x_0}{x_{\text{max}}} = 0.57 Re^{0.0417} \text{ if } x > x_{\text{max}}$			
	with $\Theta_{\text{max}} = 5$ and $x_{\text{max}} = \frac{0.4 \sqrt{g \rho_{\text{liq}} (\rho_{\text{liq}} - \rho_{\text{vap}}) d_{\text{hyd}}}}{G_{\text{tot}}} + 0.6 / \sqrt{\frac{\rho_{\text{liq}}}{\rho_{\text{vap}}}} + 0.6$			
Void Drift	Mass exchange of the phase k : $\dot{m}_k^{VD} = \beta \frac{\overline{G}}{\overline{\rho}} (\alpha_{k,j,EQ} \rho_{k,j,EQ} - \alpha_{k,i,EQ} \rho_{k,i,EQ}) A$;			
	Momentum exchange of the phase k : $\dot{I}_{k}^{VD} = \beta \frac{\overline{G}}{\overline{\rho}} \left(G_{k,j,EQ} - G_{k,i,EQ} \right) A$			
	Energy exchange of the phase k :			
	$\dot{Q}_{k}^{VD} = \beta \frac{\overline{G}}{\overline{\rho}} \left(\alpha_{k,j,EQ} \rho_{k,j,EQ} h_{k,j,EQ} - \alpha_{k,i,EQ} \rho_{k,i,EQ} h_{k,i,EQ} \right) A$			
	$\left(\alpha_{k,j,\text{EQ}} \rho_{k,j,\text{EQ}} - \alpha_{k,i,\text{EQ}} \rho_{k,i,\text{EQ}}\right) = \pm \frac{\overline{\alpha_{\text{vap}} \rho_k}}{\overline{G}_{\text{tot}}} \left(G_{\text{tot},j,\text{EQ}} - G_{\text{tot},i,\text{EQ}}\right)$			

3. TRACE Model Description

The fully conservative forms of the energy and momentum equations are modified in TRACE to provide a set of internal-energy and motion equations. This modification reduces the numerical manipulation and computational time of the solution. This modification is also transferred to the conservation of mass equation.

It is assumed that the volume average of a product is equal to the product of volume averages. Only contributions from wall heat fluxes and heat fluxes at phase interfaces within the averaging volume are normally included in the volume average of the divergence of heat flux. Also, only contributions from the stress tensor due to shear at metal surfaces or phase interfaces within the averaging volume are considered. The only portions of the work terms that contribute to change in bulk kinetic energy of motion are retained excluding viscous heating from most of the cases unless a pump component is used in which case the viscous heating from the pump to the fluid is incorporated by the term of direct-heating in the internal energy equation.

This modifications and assumptions yield a set of 6 equations of mass (Equations 7 and 8), motion (Equations 9 and 10), and internal energy (Equations 11 and 12) for gas and gas-liquid mixture. An additional mass-equation is added for non-condensable gases but in order to still solving only a single set of motion and energy equations, the non-gases are assumed to be in mechanical and thermal equilibrium with the steam.

Mass:

$$\frac{\partial \left(\alpha \rho_{g}\right)}{\partial t} + \nabla \cdot \left[\alpha \rho_{g} \vec{V}_{g}\right] = \Gamma \tag{7}$$

$$\frac{\partial \left((1 - \alpha) \rho_l + \alpha \rho_g \right)}{\partial t} + \nabla \cdot \left[(1 - \alpha) \rho_l \vec{V}_l + \alpha \rho_g \vec{V}_g \right] = 0 \tag{8}$$

Motion:

$$\frac{\partial \vec{V_l}}{\partial t} + \vec{V_l} \cdot \nabla \vec{V_l} = -\frac{1}{\rho_l} \nabla P + \frac{\left[f_i - \Gamma(\vec{V_i} - \vec{V_l}) + f_{wl} \right]}{(1 - \alpha)\rho_l} + \vec{g}$$

$$\tag{9}$$

$$\frac{\partial \vec{V}_g}{\partial t} + \vec{V}_g \cdot \nabla \vec{V}_g = -\frac{1}{\rho_g} \nabla P + \frac{\left[f_{wg} - f_i - \Gamma(\vec{V}_g - \vec{V}_i) + f_{wl} \right]}{(1 - \alpha)\rho_g} + \bar{g}$$
(10)

Internal energy:

$$\frac{\partial \left(\alpha \rho_{g} e_{g}\right)}{\partial t} + \nabla \cdot \left(\alpha \rho_{g} e_{g} \vec{V}_{g}\right) = -P \frac{\partial \alpha}{\partial t} - P \nabla \cdot \left(\alpha \vec{V}_{g}\right) + q_{wg} + q_{dg} + q_{ig} + \Gamma h_{v}'$$
(11)

$$\frac{\partial \left((1 - \alpha) \rho_l e_l + \alpha \rho_g e_g \right)}{\partial t} + \nabla \cdot \left((1 - \alpha) \rho_l e_l \vec{V}_l + \alpha \rho_g e_g \vec{V}_g \right)
= -P \nabla \cdot \left((1 - \alpha) \vec{V}_l + \alpha \vec{V}_g \right) + q_{wl} + q_{wg} + q_{dl} + q_{dg}$$
(12)

In Equations 7 and 8, the term α is the void fraction; ρ_g and ρ_l are the density of the gas and liquid respectively; V_l and V_g the velocity vectors of gas and liquid; and Γ the interfacial mass-transfer rate (positive from liquid to gas).

In Equations 9 and 10 the additional terms P is the fluid or total pressure; f_i is the force per unit volume due to shear at the phase interface; f_{wl} is the wall shear force per unit volume acting on the liquid, f_{wg} is the wall shear force per unit volume acting on the gas, V_i is the flow velocity at the phase interface, and \bar{g} is the gravity vector.

The other terms on Equation 11 and 12 are e_g and e_l which are the internal energy of the gas and liquid respectively. The terms q_{wg} and q_{wl} are the heat-transfer rate per unit volume from the wall to gas and from the wall to liquid. The terms q_{dg} and q_{dl} corresponds to the power deposited directly to the gas or liquid (without heat-conduction process). The term q_{ig} is the interfacial sensible heat transfer. The term $\Gamma h'_{v}$ account for energy carried with mass transfer at the interface, which is the products of mass transfer rate and appropriate stagnation enthalpy at the interface.

The phase-change rate in the set of equations is calculated using the heat conduction limited model (Equation 13).

$$\Gamma = \frac{-\left(q_{ig} + q_{il}\right)}{\left(h_{v}' - h_{l}'\right)} \tag{13}$$

where:

$$q_{ig} = \frac{P_{\nu}}{P} h_{ig} a_i \left(T_{s\nu} - T_{\nu} \right) \tag{14}$$

$$q_{ij} = h_{ij}a_i(T_{sy} - T_i) \tag{15}$$

The term a_i in Equations 14 and 15 is the interfacial area per unit volume, where h_{ih} and h_{il} are the heat transfer coefficients at the liquid/gas interface and T_{sv} the saturation temperature corresponding to the partial pressure P_v .

The interfacial drag forces incorporated in the motion-equations (Equations 9 and 10) is evaluated by Equation 16. The interfacial drag force is evaluated for vertical pipes and for horizontal/inclined pipes. For vertical pipes the set of correlations are calculated for Pre and

Post-critical-heat-flux (Pre & Post-CHF) condition and for

$$F_i^{\prime\prime\prime} = C_i V_r |V_r| \tag{16}$$

where C_i is the interfacial drag coefficient and V_r the relative velocity:

$$V_r = V_g - V_L$$

where

 V_g is the velocity of the gas phase and

 V_L is the velocity of the liquid phase.

The velocity of the gas-phase is evaluated using the local drift velocity (Equation 17), where j is the volumetric flux.

$$v_{gj} = V_g - j \tag{17}$$

For flow in vertical pipes under Pre-CHF conditions the interfacial drag coefficient is calculated with Equation 18 and the profile factor with Equation 19 subsequently.

$$C_{i} = \frac{\alpha (1 - \alpha)^{3} g \Delta \rho}{v_{gi}^{2}} \cdot P_{s}$$
(18)

$$P_{s} = \frac{\left(\frac{1 - C_{0}\langle\alpha\rangle}{1 - \langle\alpha\rangle}\overline{V_{g}} - C_{0}\overline{V_{l}}\right)^{2}}{V_{r}^{2}}$$
(19)

A drift flux model approach is used to evaluate local drift velocity (v_{gj}) along with the distribution coefficient (C_O) . Table III summarizes the actual drift flux models used in TRACE for small and large pipes and Bubbly/Slug and the Annular/Mist flow regimes under Pre-CHF condition.

Table III. Pre-CHF Local Drift Velocity (v_{gj}) and Distribution Coefficient (C_0)

	Dispersed Bubbly Flow	Transition	Dispersed Bubbly Flow
	$(0 < \alpha < 0.2)$	$(0.2 < \alpha < 0.3)$	$(0.3 < \alpha < 0.5)$
Small Pipes	Ishii's Eq. (1997)	Interpolation	Kataoka-Ishii's Eq.(1987)
Dh < 0.18			
Large Pipes	Ishii's Eq. (1997)	Interpolation	Kataoka-Ishii's Eq.(1987)
Dh > 0.18			

For post-CHF conditions three principal inverted flow regimes are modeled in TRACE, which are inverted annular, inverted slug, and dispersed flow. These three regimes are defined in terms of void fraction and gas superficial velocity.

The inverted-annular regime is used in TRACE for void fractions below 0.6 and the interfacial drag coefficient is calculated using Equation 20.

$$C_{i,IA} = \frac{1}{2} \rho_g f_i A_i^{"} \tag{20}$$

Inverted slug regime is used in TRACE for a void fraction between 0.6 and 0.9 and the dispersed flow for a void fraction over 0.9. In both regimes the interfacial drag coefficient is calculated with Equation 21, where $C_{D,MP}$ is the drag coefficient for multi-particles and A_p^m is the projected area per unit volume. The projected area is calculated differently for each regime.

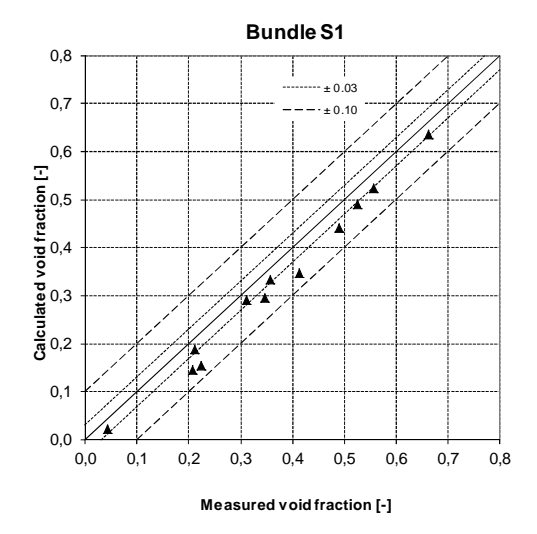
$$C_i = \frac{1}{2} \rho_g C_{D,MP} A_p^{"} \tag{21}$$

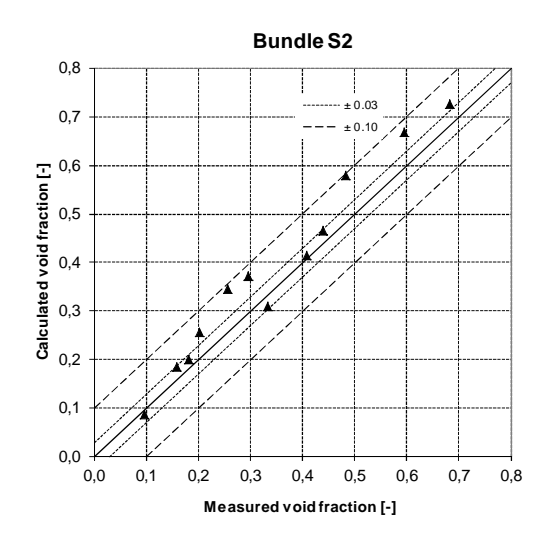
4. CTF and TRACE Applications to the Void Distribution Phase of the OECD/NRC PWR Subchannel and Bundle Tests Benchmark

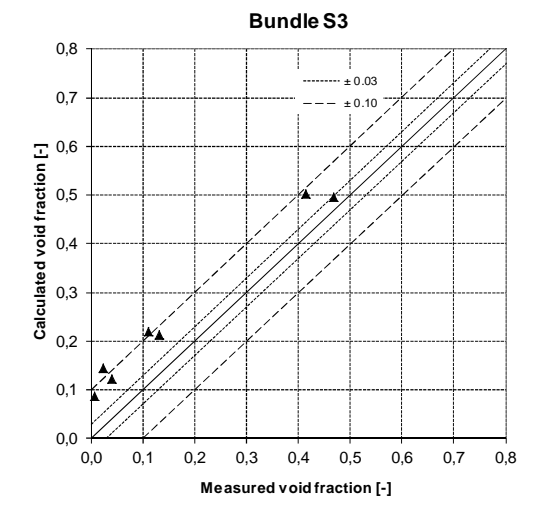
The test cases of Exercise I-1 were calculated with CTF for four bundle types – S1, S2, S3, and S4. Only the heated length of the subchannel was modeled in an axial discretization of forty equidistant nodes. Code-to-data comparisons are given in Figure 1. It can be seen that the CTF predictions stay within the error bound of 10% void (the experimental uncertainties for the steady state void fraction CT scanner measurements were specified as 3% void). This is in an agreement with a previously observed tendency of CTF to overpredict the vapor generation rate [9].

Eight tests of the steady state series-5 (5×5 bundle B5) were modelled by TRACE and CTF. The heated section of the bundle is model in TRACE with a three dimension component discretized in 23 axial nodes, 2 radial nodes and 1 azimuthally node assuming the power distribution is axis-symmetrical. As it can be observed in Figure 2, TRACE predicted the void fraction at the upper part of the bundle with an average error of 2% and maximum error of 7%. In the middle part of the bundle TRACE predicted the void-fraction with an average error of 8% and a maximum of 13%. On the other hand for the lower part of the bundle TRACE over-predicted the void fraction with an average error of 10% and a maximum 16%. The entire B5 bundle was modelled by CTF in a subchannel-by-subchannel basis - no symmetry was used. The heated length was divided axially into seventy equidistant nodes. The pressure losses due to spacer grids were calculated as velocity head losses with a loss coefficient of 1.0. The total cross-flow between two adjacent subchannels was simulated as a sum of the diversion cross-flow due to lateral pressure gradients and the lateral flow due to turbulent mixing and void drift. The steady state void fraction predictions by CTF show very similar, but slightly better agreement with the measurements as compared to TRACE.

Power increase, flow reduction, depressurization, and temperature increase transients were simulated by NUPEC and selected as benchmark exercise cases. The space-averaged instantaneous axial void fraction profiles during the transients were supplied for code-to-data comparisons. The X-ray densitometers measurements were taken at three intermediate elevations along the heated length: 2216 mm, 2669 mm, and 3177 mm. The four transients were simulated with CTF and TRACE for the bundle type B5. Both codes utilised the same configurations used in the steady state cases. As previously mentioned in TRACE the heated length was divided in 23 axial nodes, where 17 of those nodes upper-faces are located at the same elevation of the spacer grids, which pressure drops are incorporated into the model with a k factor of 1 as well. CTF and TRACE results are given in Figure 3. The experimental uncertainties were specified as 5 % void. As seen in Figures $3 \div 6$, both codes are capable of reproducing the transient behavior of the bundle average void fraction for the four transient scenarios. The agreement is better at higher axial elevations. The time shift observed in the temperature increase transient for both codes should be attributed to the heat capacitance effect of the downcomer region.







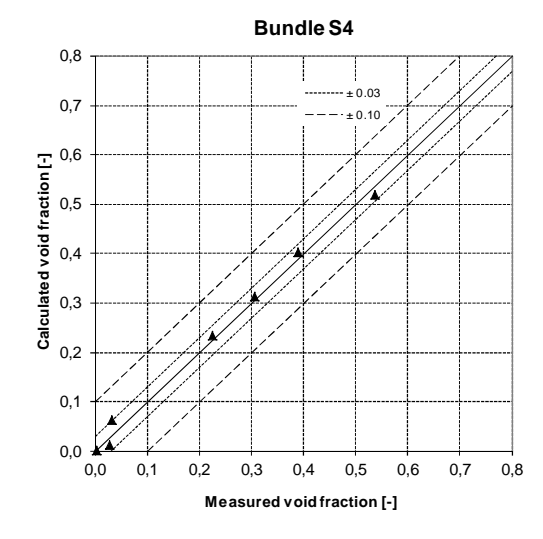


Figure 1. CTF Predictions of Steady State Void Fraction in Single Subchannel Tests

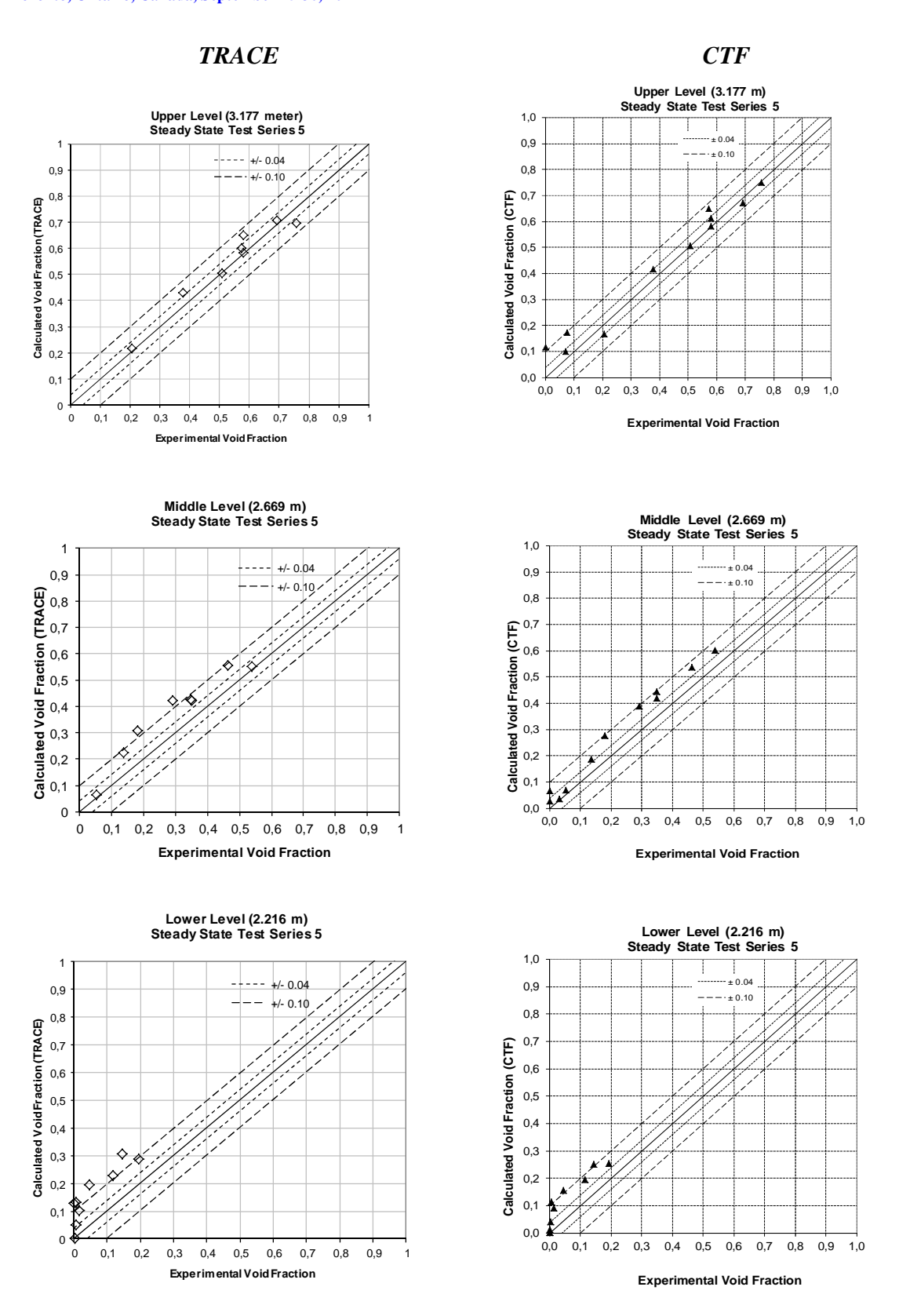


Figure 2. TRACE and CTF Predictions of Steady State Test Series 5 of the 5×5 bundle B5

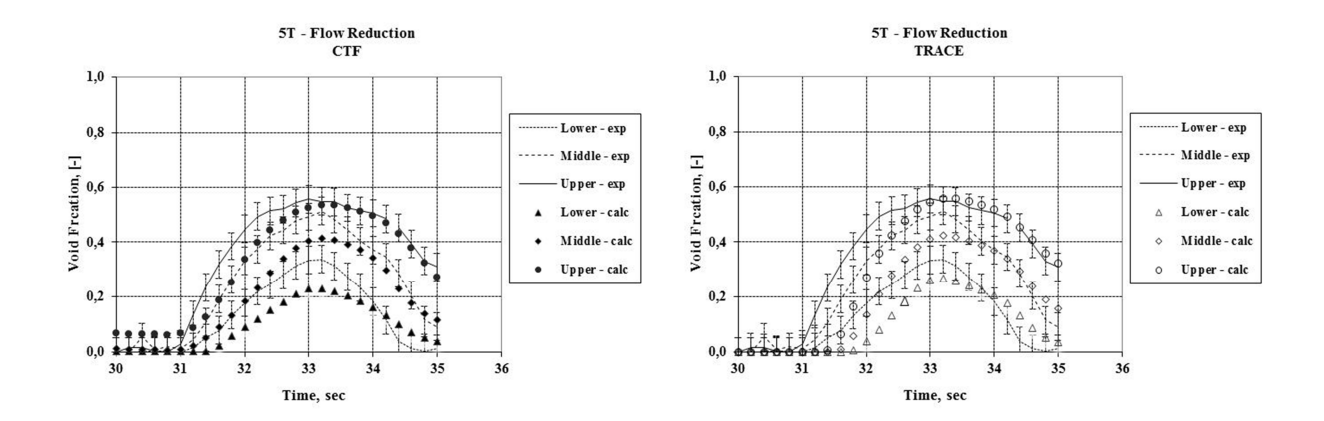


Figure 3. CTF (left) and TRACE (right) Predictions of Void Fraction in Bundle Type B5 during Flow Reduction Transient

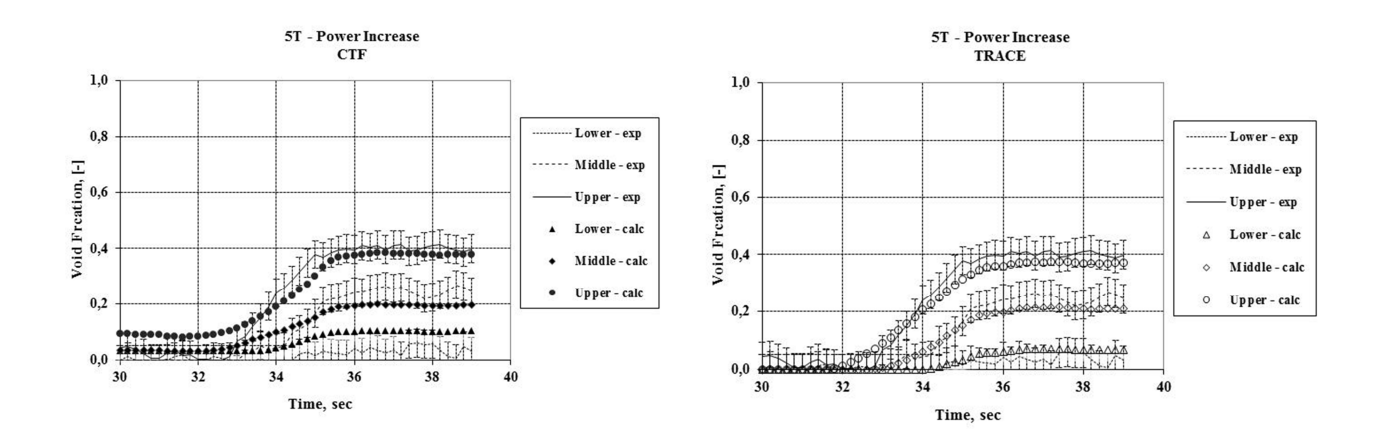


Figure 4. CTF (left) and TRACE (right) Predictions of Void Fraction in Bundle Type B5 during Power Increase Transient

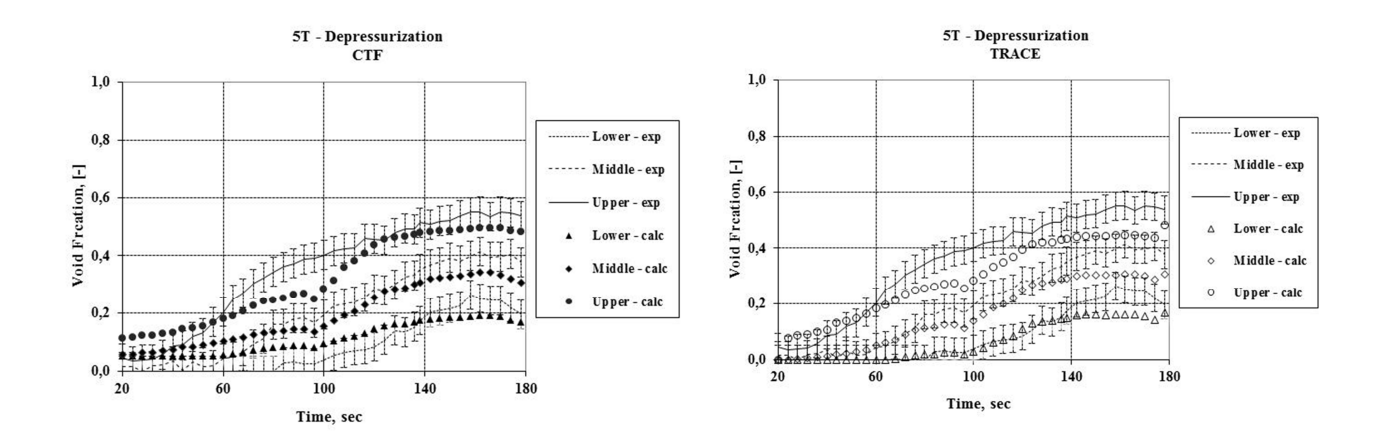


Figure 5. CTF (left) and TRACE (right) Predictions of Void Fraction in Bundle Type B5 during Flow Depressurization Transient

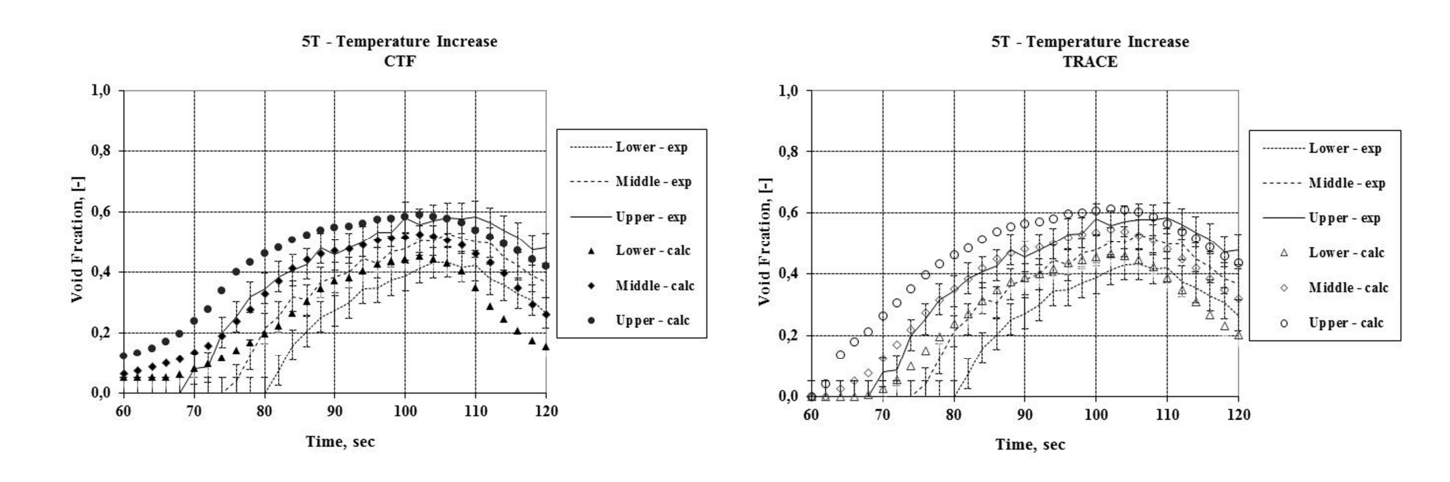


Figure 6. CTF (left) and TRACE (right) Predictions of Void Fraction in Bundle Type B5 during Temperature Increase Transient

7. Conclusions

On behalf of the OECD/NRC PSBT benchmark team, PSU in collaboration with US NRC is performing supporting calculations of the benchmark exercises using its in-house advanced thermal-hydraulic subchannel code CTF and the US NRC system code TRACE. CTF and TRACE were applied to the steady state and transient void distribution cases. Both codes were able to reproduce the measured data in a good agreement.

8. References

- [1] A. Rubin, et al., "OECD/NRC Benchmark Based on NUPEC PWR Subchannel and Bundle Tests (PSBT). Volume I: Experimental Database and Final Problem Specifications", NEA/NSC/DOC(2010)1, January 2010
- [2] "CTF A Thermal-Hydraulic Subchannel Code for LWRs Transient Analyses. User's Manual", Technical Report, RDFMG, The Pennsylvania State University, 2009
- [3] C. Y. Payk et al., Analysis of FLECHT SEASET 163-Rod Blocked Bundle Data using COBRA-TF, NRC/EPRI/Westinghouse-12 (1985)
- [4] M. Avramova, et al., "Improvements and Applications of COBRA-TF for Stand-Alone and Coupled LWR Safety Analyses", Proceedings: PHYSOR-2006, Vancouver, Canada, September 2006
- [5] TRACE V5.0 Theory Manual. Field Equations, Solution Methods, and Physical Models, USNRC, Washington DC
- [6] R. T. Lahey and F. J. Moody, The Thermal Hydraulics of a Boiling Water Nuclear Reactor, American Nuclear Society (ANS) (1993)
- [7] J. T. Rogers and R. G. Rosehart, Mixing by Turbulent Interchange in Fuel Bundles, Correlations and Inferences, ASME, 72-HT-53, (1972)
- [8] S. G. Beus, A two-phase turbulent mixing model for flow in rod bundles. Bettis Atomic Power Laboratory, WAPD-T-2438, (1970)
- [9] M. Avramova, et al., "Analysis of Void Distribution Predictions for Phase I of the OECD/NRC BFBT Benchmark using CTF/NEM", Proceedings: NURETH-12, Pittsburgh, Pennsylvania, USA, September 2007